Electrical Power and Energy Systems 145 (2023) 108630

Contents lists available at ScienceDirect

International Journal of Electrical Power and Energy Systems

journal homepage: www.elsevier.com/locate/ijepes

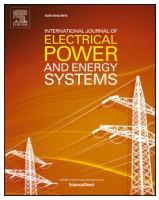

Integration of superconducting fault current limiter with solid-state DC circuit breaker

Jiawen Xi [a,b], Xiaoze Pei [b,*], Wenjuan Song [c], Liyong Niu [d], Yuhan Liu [e], Xianwu Zeng [f]

[a] China Huaneng Clean Energy Research Institute, Future Science Park, Beijing, 102209, China
[b] Department of Electronic and Electrical Engineering, University of Bath, Bath, BA2 7AY, UK
[c] James Watt School of Engineering, University of Glasgow, Glasgow, G12 8QQ, UK
[d] School of Electrical Engineering, Beijing Jiaotong University, Beijing, 100044, China
[e] Energy Research Department, Electric Power Development Research Institute, Beijing, 100053, China
[f] Department of Mechanical Engineering, University of Bath, Bath, BA2 7AY, UK

ARTICLE INFO

Keywords:
Circuit breaker testing
DC circuit breaker
Electric aircraft
SFCL
Solid-state circuit breaker

ABSTRACT

The onboard direct current (DC) system in electric aircraft could face a severe fault current, which is tens of times the nominal current in a short-circuit fault. It is critical to limit the fault current and clear the fault within a few milliseconds to prevent any damage to the DC system. A protection method using a resistive superconducting fault current limiter (SFCL) with a solid-state DC circuit breaker (SSCB) to manage the DC short-circuit fault is proposed and experimentally verified. A bifilar SFCL coil prototype with two types of connection to achieve low and high inductance is designed and tested, which reduces the fault current considerably from 2000 A to below 1000 A. The performance when integrating the low and high inductance SFCL with a solid-state DC circuit breaker are investigated. It is found that when integrating the SFCL with the SSCB, a high voltage is induced across the high inductance SFCL during current interruption tests. In terms of reliability and durability, the low inductance SFCL is preferred to integrate with the SSCB. The experimental results show that the low inductance SFCL can be an effective solution to protect the DC system from severe fault currents and then SSCB can rapidly and reliably interrupt the fault current at 1000 A.

1. Introduction

Climate change caused by greenhouse gas emissions is a growing worldwide environmental concern. On the path towards reducing the global carbon footprint and achieving zero carbon emissions, improving energy efficiency and increasing electricity consumption from clean energy resources rather than fossil fuels are two major avenues to achieve these targets. Ensuring flexible, safe and reliable power transmission and distribution are important aspects for expanding clean energy and electrification uptake.

The electric aircraft is a promising candidate to reduce the carbon footprint. This is because electric aircraft has lower environmental impact, higher efficiency, less fuel consumption and potential mass savings. A DC distribution system has been proposed as a feasible solution to increase fuel efficiency, provide flexibility in the operation of the electrical system, and ensure highly reliable power supplies for turboelectric aircraft [1,2]. In electric aircraft, the DC bus voltage is only a few hundred volts [3–5]. However, because the DC system has extremely low impedance, the peak value of a fault current can be tens of times the rated current, and can be achieved within several milliseconds during a short-circuit fault [6]. This significantly high rate of rise of the fault current leads to more critical requirements for the response speed and interruption speed of DC circuit breakers (DCCBs). For example, a slow response and interruption speed means that a higher fault current level will be reached and lead to potentially seriously damaging equipment, fire, etc. Therefore, a circuit breaker with a fast interruption speed and better fault clearing capability is required. Among all the types of DCCBs, solid-state circuit breakers (SSCBs) have the fastest interruption speed in tens of microseconds and possess a long service life [7–11], and are suitable for electric aircraft.

To deliver effective protection performance in a DC system, integrating a DCCB with a superconducting fault current limiter (SFCL) is a

* Corresponding author.
E-mail address: x.pei@bath.ac.uk (X. Pei).

https://doi.org/10.1016/j.ijepes.2022.108630
Received 7 May 2022; Received in revised form 15 July 2022; Accepted 4 September 2022
Available online 21 September 2022

potential solution. A fault current can be reduced by an SFCL to an acceptable level, and then be interrupted by a DC circuit breaker. A superconductor exhibits zero DC resistivity in the superconducting state during normal operation, and rapidly produces a resistance to suppress a fault current once it is quenched. Thus, superconductors offer intrinsic fault tolerance capability during a fault [12]. With these characteristics, therefore, a superconducting fault current limiter (SFCL) is able to limit the short-circuit current level during a fault without introducing any impedance into a DC system during normal operation. Resistive type SFCLs (R-SFCLs) have attracted a lot of research interests due to compact and simple topologies, and better current limiting performance than other types [13,14]. In recent years, most of the research and development SFCL projects focus on the resistive type [15,16]. A 20 kV/400 A solenoid R-SFCL was developed for a ± 10 kV voltage source converter (VSC) DC system at Suzhou Nami substation, which consists of 8 series-connected solenoid coils. It successfully passed the test to limit a prospective fault current of 8 kA to 2.26 kA in 2019 [17]. A 40 kV/2 kA SFCL has been designed and tested by Chinese Academy of Sciences, which consists of 24 solenoid coils (6 branches and each branch contains 4 series-connected coils) using 800 m yttrium barium copper oxide (YBCO) tapes [18]. The series–parallel structure is used in HVDC system, and the inductance of the SFCL can be controlled by adjusting the mutual inductance. A 160 kV/1 kA R-SFCL prototype based on rare-earth barium copper oxide (REBCO) tapes has been developed for the Nan'ao ± 160 kV HVDC transmission system in China [19,20]. This R-SFCL consists of 24 pancake coils. As inlet turns are close to outlet turns, the insulation structure must be carefully designed, and insulation performance must be experimentally tested. A mechanical circuit breaker with R-SFCL has been proposed and tested by Xi'an Jiaotong University [21–23], which successfully limited a 10 kA fault current to 1.57 kA and interrupted the current in around 16 ms. A hybrid direct current circuit breaker with R-SFCL has been designed and investigated by the University of Manchester, which interrupted a 500 A direct current in 4.4 ms after a fault [24]. However, the interruption speeds of the above circuit breakers are not suitable for electric aircraft. Hence, it is critical to develop a reliable protection solution with an ultrafast interruption speed.

In this paper, a protection method which integrates resistive SFCL and SSCB is proposed and investigated. Firstly, the design of SFCL coil with two connection methods and DC SSCB prototype is introduced. Secondly, the current limiting performances of the SFCL coil using two connection methods are experimentally investigated and compared. Finally, the SFCL prototype integrating with the SSCB prototype is experimentally studied using different operating modes.

2. Design of SFCL and SSCB

A DC protection solution using an SFCL integrated with a DC SSCB is proposed. Once a fault happens, the SFCL could respond within 1 ms to suppress the current rise and the peak of the fault current to a lower amplitude, and then the SSCB interrupts the fault current in an ultrafast speed. The ultrafast interruption speed means that the fault current level and fault energy can also be reduced significantly.

2.1. SFCL design

A helical bifilar SFCL coil, as shown in Fig. 1, wound by 12 mm wide AMSC type 8602 high temperature superconduting (HTS) tape has been proposed and tested in previous work [25,26]. Considering that a voltage up to 300 V is applied to the SFCL coil, a 7.5 m long superconducting tape is used to wind the coil. The length of the superconducting tape is selected considering the electric field per meter and the quench resistance. The electric field of a superconducting tape is limited to around 50 V/m for AC short circuit of 60 ms [23,27,28] and can be increased to 300 V/m for DC short circuit of 10 ms [29] in order to protect the superconducting tape from overheating. The electric field of the superconducting tape is less than 40 V/m for this case. The SFCL coil is composed of two superconducting tape layers wound onto one G10 tube in opposite directions with a 15.5 mm pitch, namely an inner winding layer and an outer winding layer, respectively. Voltage taps are soldered close to both ends of each superconducting tape layer to measure the voltage drops across the SFCL coil. The inner winding layer is wound in the clockwise direction. Kapton tape is used to provide insulation between the two superconducting tape layers. Finally, the outer winding is wound in the anti-clockwise direction and insulated by another layer of Kapton tape. A group of nylon studs are placed on the bobbin to assist in locating the HTS tapes. Four terminal connections are placed on both ends of the G10 tube, each of the superconducting tape terminals is fixed by two copper plates with thin indium foil inside. Table 1 lists the SFCL coil key parameters.

With different terminal connections, the SFCL coil inductance is different, namely a low inductance type and a high inductance type. Fig. 2 shows the terminal connections for the low inductance coil and the high inductance coil. The solid helical line represents the outer winding and the dotted helical line represents the inner winding. In Fig. 2 (a), Terminals 2 and 3 are connected to form the coil with a low inductance. Furthermore, Terminal 1 is connected to the system as the current inlet whereas Terminal 4 is the current outlet. The value of inductance for the low inductance coil can be calculated as:

$$L = L_1 + L_2 - 2M \tag{1}$$

where L_1 and L_2 represent the inner winding and the outer winding self-inductances, respectively, and M denotes the mutual inductance

Table 1
SFCL coil specifications.

Items	Inner winding	Outer winding
Winding direction	Clockwise	Anti-clockwise
Inner diameter	89 mm	89.6 mm
Number of turns	12	13
Pitch	15.5 mm	15.5 mm
Insulation	Kapton	Kapton
Distance between voltage taps	350 cm	375 cm

Fig. 1. Helical bifilar SFCL coil.

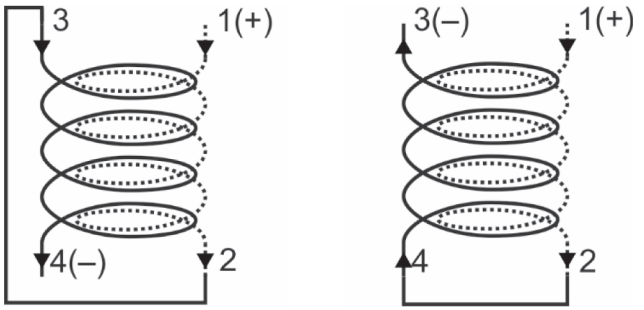

(a) Low inductance (b) High inductance

Fig. 2. Schematic diagrams of the SFCL coil terminal connections for the inner (dotted helical) and outer windings (solid helical).

between the two windings.

In Fig. 2 (b), Terminals 2 and 4 are connected to make the coil exhibit a high inductance, and Terminal 3 becomes the current outlet. The value of inductance for the high inductance coil can be calculated as:

$$L = L_1 + L_2 + 2M \quad (2)$$

The inductance and resistance at room temperature (RT) for both the low and high inductance connections are listed in Table 2. The inductances are measured using an LCR meter. The SFCL coil inductance in Fig. 2 (a) is 2.65 μH, and in Fig. 2 (b) is 23.93 μH. The SFCL coil inductance with high inductance connection is nine times that of the value with low inductance connection. The resistances at room temperature of both the inner and outer windings are measured using a four-wire measurement method [30]. The room temperature resistance of the inner winding is measured to be 385 mΩ, and that of the outer winding is measured to be 405 mΩ, therefore, the room temperature resistance of the inner winding is 110 mΩ/m and the outer winding is 108 mΩ/m.

Table 3 presents the critical current (Ic) of the SFCL coil for low inducance and high inductance connections. With the low inductance connection, the critical currents of both the inner and outer windings are almost identical at 253 A. However, with the high inductance connection, the critical currents of the two windings are different. The critical current of the inner winding is 238 A, whereas the value of the outer winding is 247 A. Due to the higher inductance, both of the measured values are lower compared with those measured for the low inductance connection. In addition, the magnetic field applied to the inner winding is higher and therefore the critical current is lower than the outer winding.

2.2. SSCB prototype

A solid-state direct current circuit breaker using series connected and parallel connected IGBTs is designed to interrupt DC current. Fig. 3 shows the photo and topology of the SSCB prototype. Two IGBT modules are fixed on a large heatsink. Metal oxide varistors (MOVs) are conneted to IGBT modules through customised copper bars. A voltage balancing circuit board and an IGBT gate drive circuit board are placed as close as possible to IGBT modules. The detailed topology and design can be found in [11,31].

To control the operation of the SSCB prototype, a control PCB board associated with the IGBT gate drive PCB board is designed to send a turn-on or turn-off signal to the SSCB. Fig. 4 illustrates the structural diagram

Table 2
Parameters of the SFCL coil.

Connection	SFCL coil inductance @ RT	Resistance @ RT	
		Inner winding	Outer winding
Low inductance	2.65 μH	110 mΩ/m	108 mΩ/m
High inductance	23.93 μH		

Table 3
Critical current of the SFCL coil.

Connection	Critical current Ic @ 77 K	
	Inner winding	Outer winding
Low inductance	253 A	253 A
High inductance	238 A	247 A

of the control block. The control block has three operating modes: 1) Mode 1, the ON and OFF states of the SSCB are controlled manually by using "CLOSE" and "OPEN" switches; 2) Mode 2, the SSCB is turned on using the "CLOSE" switch and then turned off after a pre-set delay time; 3) Mode 3, the SSCB is turned on using the "CLOSE" switch and when the current flowing through the SSCB is higher than a pre-set level, the overcurrent protection can be automatically triggered to turn off the SSCB with minimum delay. An external LEM current transducer is added and connected to the control PCB board for current detection. In addition, an OLED display on the control PCB board is implemented to show key parameters and information, such as the detected current level and the SSCB status.

3. Experimental testing and result analysis

3.1. Testing circuit setup

Fig. 5 presents the schematic diagram of SFCL with SSCB in a DC fault test rig. The test rig utilises an inductor-capacitor resonant circuit to generate short-circuit fault currents in electric aircraft DC network. The 12 mF capacitor C1, which represents the DC bus capacitor in the electric aircraft, can be charged through a direct current power source DC1 when the switch S1 is closed. When the voltage level of C1 reaches a design value, S1 can be opened. Inductor L1 is a 60 μH air-core inductor, which is the same order of magnitude as the value of high inductance SFCL coil. A shunt resistor Rsh is connected to the circuit to measure current level, and a diode D1 is placed to stop C1 from reverse charging.

Fig. 6 presents the experimental setup in the laboratory. The SFCL coil is immersed in the LN_2 bath, and is connected between the inductor and the inlet of the SSCB prototype. The LEM current transducer is used to convert the current signals into voltage signals, which are detected by the control board, through the Hall Effect.

3.2. Prospective fault current tests

The prospective fault current values were tested under different capacitor voltage levels. The inductor L1 was connected to the SSCB directly in Fig. 5. The capacitor C1 was charged to a designed voltage and the SSCB acted as a switch to trigger the circuit and generate a fault current without any interruption operation. The voltage was set from 10 V to 100 V in 10 V increments, to generate different prospective fault currents. Both the capacitor voltage and the fault current were recorded. A prospective current reached 1008 A when the capacitor was pre-charged to 100 V. For higher voltage levels, the prospective fault currents are estimated based on a linear trendline of the experimental results, as illustrated Fig. 7.

3.3. Current limiting performance tests

3.3.1. Current limitation by the high inductance SFCL coil

To produce the high inductance SFCL, the terminals of the SFCL coil were connected as shown in Fig. 2 (b). Terminal 1 was connected to the inductor L1 and Terminal 3 was connected to the SSCB. The current limiting performances were studied under prospective fault currents up to 2048 A (capacitor voltage of 200 V).

The experimental results with prospective fault current peak values of 280 A and 2048 A are shown in Fig. 8 and Fig. 9. The grey line in the

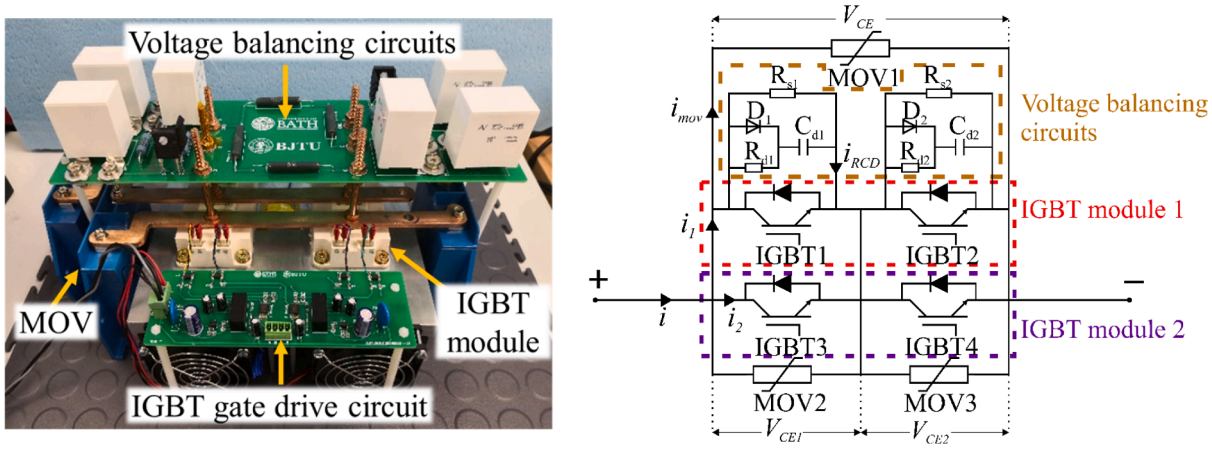

(a) SSCB photo (b) SSCB topology

Fig. 3. Photo and topology of the SSCB.

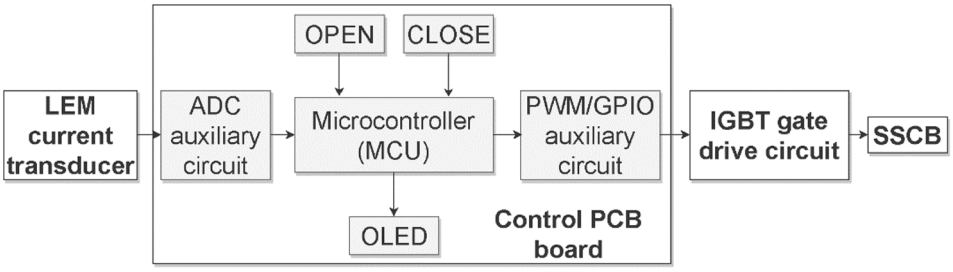

Fig. 4. Structure diagram of the control block.

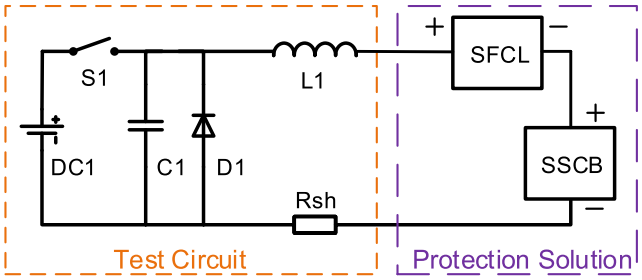

Fig. 5. DC fault test circuit and proposed protection solution.

figures represents the prospective fault current (without SFCL), and the orange line represents the current using the SFCL coil (with SFCL). The blue and purple lines show the inner winding voltage drop (Vinner) and outer winding voltage drop (Vouter), respectively. The green line is the capacitor C1 voltage (Vcap).

As shown in Fig. 8, when the capacitor C1 is pre-charged to 30 V, the prospective peak fault current is 280 A, which is slightly higher than the SFCL coil critical current. The fault current is reduced to 252 A by the SFCL coil. In addition, the time for peak fault current (tpeak) is extended from 1.33 ms to 1.56 ms, because of the presence of the high inductance of the SFCL coil. At the beginning of the fault, a total voltage of 7.5 V across both the inner and outer windings is measured, which is induced by the inductance of the SFCL coil.

In Fig. 9, the capacitor C1 was pre-charged to 200 V, and the prospective fault current peak value is more than eight times higher than the SFCL coil critical current. The SFCL coil limits the fault current from 2048 A to 928 A using its inductance and quench resistance, which means that the fault current reduction ratio is 55%. The quench resistence results in the peak time tpeak reducing to approximately 0.82 ms.

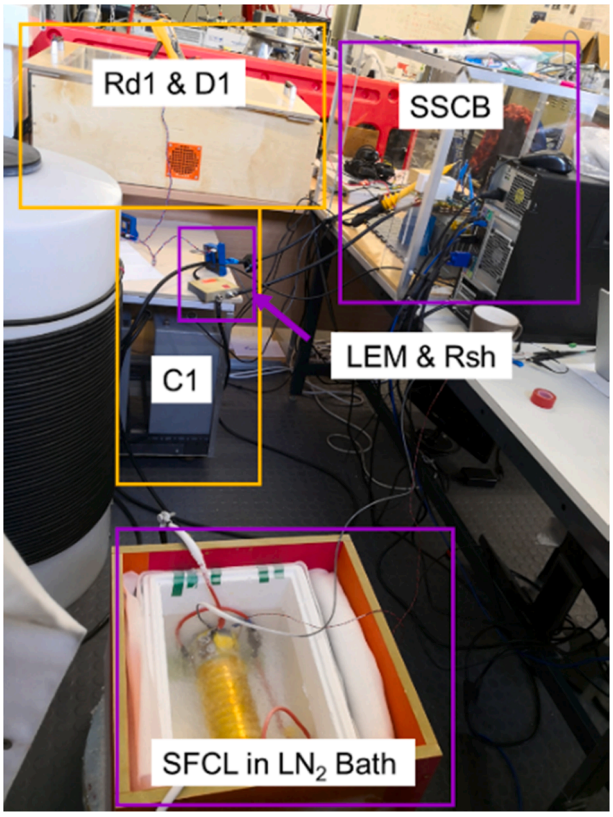

Fig. 6. Experimental setup for the SSCB and SFCL coil tests.

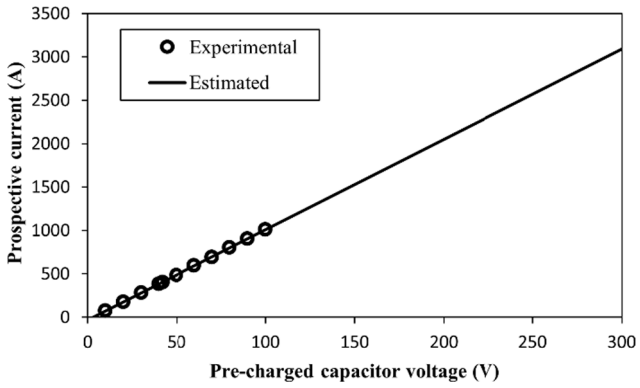

Fig. 7. Prospective fault current peak value as a function of the capacitor pre-charge voltage level.

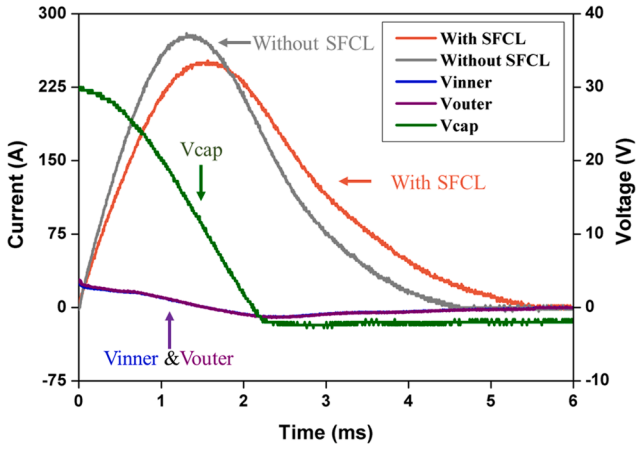

Fig. 8. High inductance SFCL current limiting performance with prospective fault current of 280 A (pre-charged capacitor voltage of 30 V).

As seen in Fig. 9 (a), a voltage spike induced by the high inductance of the SFCL coil appears following the fault. Hence, the SFCL coil inductance should be cautiously considered to prevent any damaging voltage across the SFCL coil from exceeding the dielectric capability of the insulation of SFCL coil itself and the cryostat cooling system. The second voltage spike at around 0.9 ms is produced by the quench resistance of the SFCL coil. In Fig. 9 (b), it can be observed that the quench resistance of the inner winding (Rinner) is greater than that of the outer winding (Router). This means that a quench of the inner winding is more obvious, which is caused by the worse cooling effect and the lower critical current level of the inner winding.

3.3.2. Current limitation by the low inductance SFCL coil

The terminals of the SFCL coil were connected based on Fig. 2 (a) for the following tests, to achieve the low inductance connection structure. Terminal 1 was connected to the inductor and Terminal 4 was connected to the SSCB. The current limiting performances were studied under the prospective fault currents up to 2048 A (capacitor voltage of 200 V).

In Fig. 10 (a), the capacitor C1 was charged to 200 V, and the estimated prospective fault current peak value is eight times as large as the critical current. The SFCL coil limits the fault current from 2048 A to 976 A less than a half. In Fig. 10 (b), the outer winding recovers to the superconducting state when the current is reduced to 200 A and then the inner winding recovers at 180 A. Due to the larger contact area with liquid nitrogen (LN_2), the cooling effect of the outer winding is better, which consequently observes a quicker recovery time.

3.3.3. Comparison between the two inductance connections

Fig. 11 summarises the maximum current levels with and without the two types of the SFCL coil when the capacitor is pre-charged from 10 V up to 200 V. The prospective current peak value without the SFCL coil (solid line) increases linearly with the pre-charge voltage of the capacitor. After introducing the SFCL coil, the current amplitude decreases obviously when the capacitor voltage is higher than 50 V (corresponding to a prospective fault current of 484 A). The current limitation of the SFCL coil is similar under both low and high inductance connection methods. The SFCL coil under both connections can suppress the fault current of 2048 A to less than 1000 A.

The SFCL coil current limitation ratio and the maximum quench resistance of both windings under the low inductance and high inductance connection methods at different prospective fault currents are presented in Fig. 12. The solid line with circle markers (Limit_low) and dashed line with triangle markers (Limit_high) represent the current limiting levels using the low inductance SFCL coil and the high inductance SFCL coil, respectively. Hollow circle markers (Rinner_low) and solid circle markers (Router_low) show the quench resistances in milliohm per meter for the inner and outer windings with the low inductance connection, respectively, whilst the hollow triangle markers (Rinner_high) and solid triangle markers (Router_high) stand for the quench resistances in milliohm per meter of the inner winding and outer winding with the high inductance connection, respectively.

There is almost no current reduction when the prospective fault current is lower than the critical current Ic (253 A) for the low inductance SFCL coil. It only starts to reduce the fault current and to exhibit a

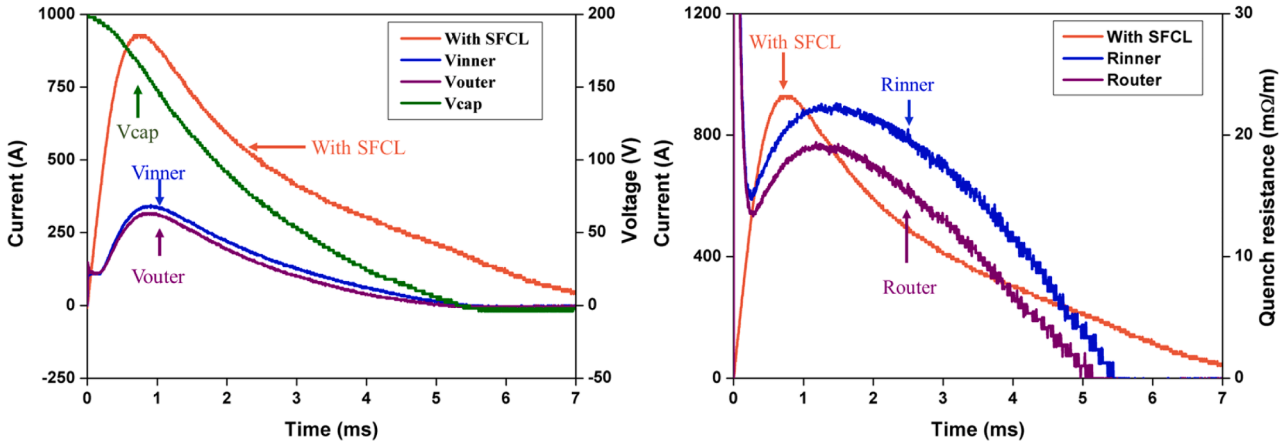

(a) Fault current and voltage drops (b) Fault current and quench resistances

Fig. 9. High inductance SFCL current limiting performance with prospective fault current of 2048 A (pre-charged capacitor voltage of 200 V).

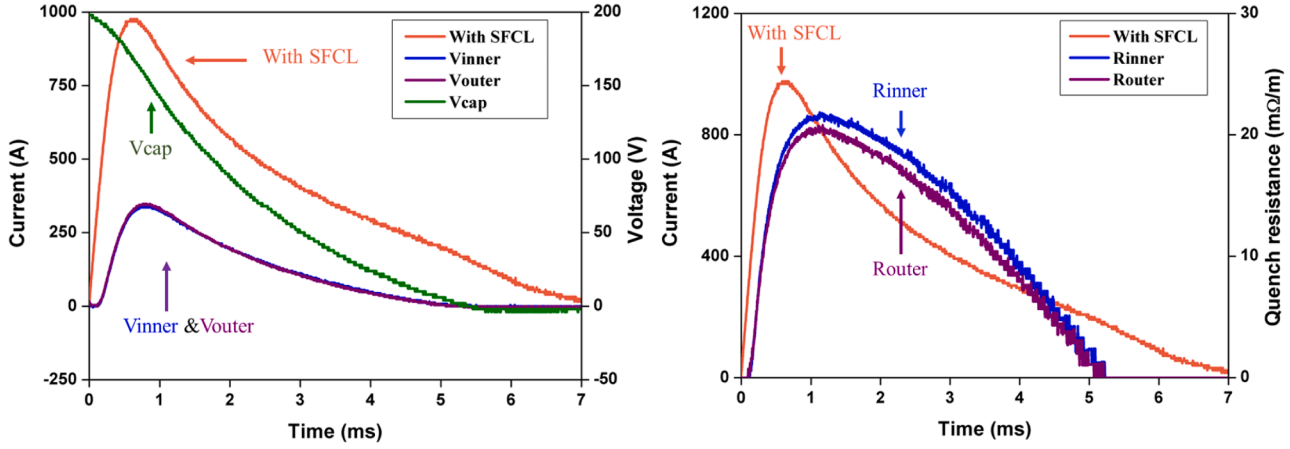

(a) Fault current and voltage drops (b) Fault current and quench resistances

Fig. 10. Low inductance SFCL current limiting performance with prospective fault current of 2048 A (pre-charged capacitor voltage of 200 V).

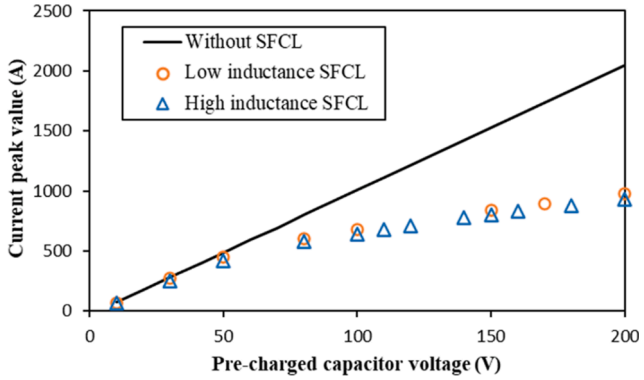

Fig. 11. Maximum current values using different capacitor pre-charge voltage levels.

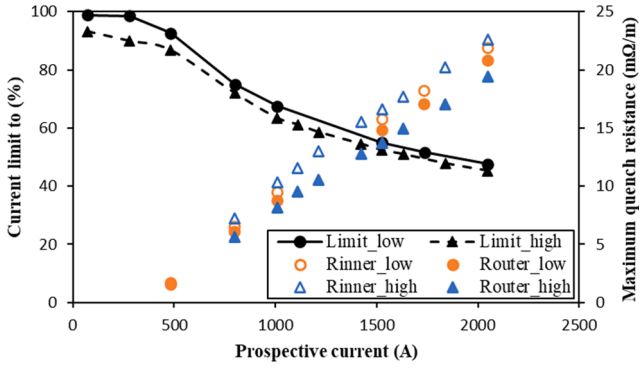

Fig. 12. Current limitation ratio and maximum quench resistance against prospective fault current.

quench resistance when the fault current is higher than the critical current. The SFCL coil with the high inductance connection has a certain current limitation even when the prospective fault current is lower than the critical current. It is because the effect of high inductance on delaying the change of short-circuit current will be stronger even in the superconducting state. The delay effect of the inductance plays an important role in limiting fault current rise rate and fault current peak when the prospective fault current is lower than two times super-contuing tape critial current. As the prospective fault current increases higher than two times critial current, the quench resistance performs greater impact on limiting the fault current. For both connection methods, as the prospective current increases, the SFCL coil develops higher quench resistance and limits the fault current more effectively. In addition, the difference in the current limiting ratios of the two connection methods becomes smaller as the prospective fault current increases. This means that the effect of the inductance becomes smaller, and the quench resistance dominants the current limiting performance.

3.4. *Current interruption tests*

Two operating modes (Mode 2 and Mode 3) of the control block are applied to the SSCB prototype for the current interruption tests. By using the Mode 2, a turn-on signal with a fixed duration is sent to the SSCB prototype after manually triggering the “CLOSE” switch on the control board. This operating mode is used to compare the performance of the SFCL coil with the two different inductance connections during the interruption of the SSCB prototype. The fixed duration is assumed to be the potential detection time of the SSCB prototype. By using the Mode 3, the control block adds an overcurrent detection function to interrupt the current automatically. The use of this operating mode aims to evaluate the detection method and the coordination between the SFCL and the SSCB prototype.

3.4.1. *SSCB prototype combined with the high inductance SFCL coil*

The SSCB prototype combined with the high inductance prototype SFCL coil was connected to the DC fault test circuit. The capacitor was pre-charged to 200 V. The control block was set to Mode 2 when the fault curent is interrupted at 1 ms. After commencing the test at 0 ms, the SSCB prototype was programmed to clear the fault current at 1 ms in Fig. 13. The orange line denotes the current measured by the shunt resistor Rsh (with SFCL), and the green line represents the voltage drop across the SSCB prototype (VCE). The blue and purple lines show the inner winding voltage drop (Vinner) and outer winding voltage drop (Vouter), respectively.

During the current interruption test, the voltage oscillations of both windings are caused by the variation of quench resistance between the two windings. The maximum voltages reach −226 V for the inner winding and −252 V for the outer winding, respectively. Therefore, the high inductance SFCL coil experiences a negative voltage of more than 64 V/m, which may exceed the dielectric strength of the coil [23,27,28]. Some measures should be taken to protect the SFCL coil from high voltage during an interruption. These high voltages are induced by the SFCL coil inductance and the rapid change of the fault current. To interrupt a fault current at an extremely fast speed, the rate of change of the current will be high. The SSCB prototype with the high inductance SFCL coil can interrupt the fault at 880 A within 50 μs, however, the

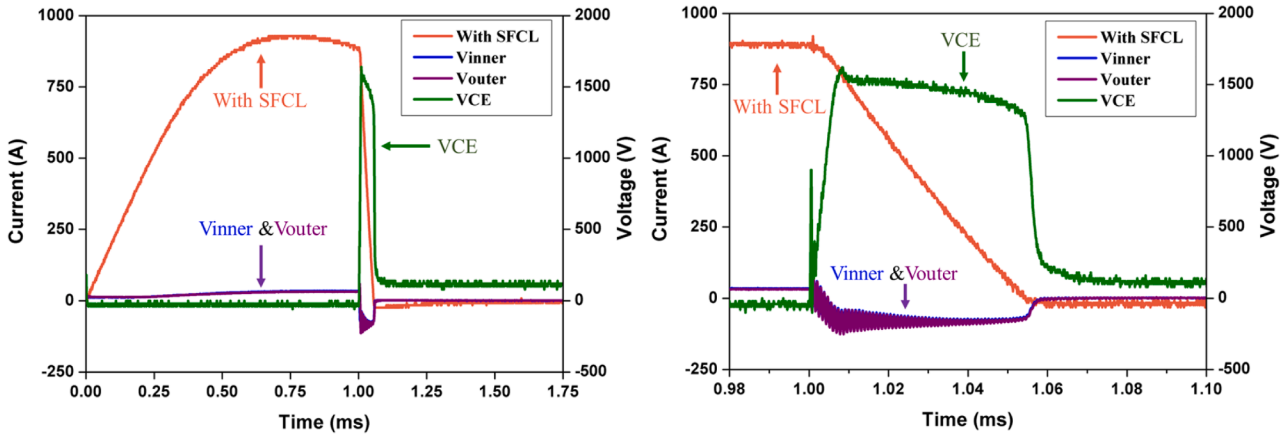

(a) Whole period (b) Zoom in during interruption

Fig. 13. Current interruption performance of the SSCB prototype with the high inductance SFCL coil at 880 A (pre-charged capacitor voltage is 200 V and the SSCB prototype is turned off at 1 ms).

voltage induced across SFCL by the inductance has to be designed carefully, in particular for high voltage application.

3.4.2. SSCB prototype combined with the low inductance SFCL coil

The SSCB prototype combined with the low inductance SFCL coil was connected to the DC fault test circuit. In Fig. 14, the capacitor was pre-charged to 200 V. The control block was also set to Mode 2. At 0 ms, the SSCB prototype was turned on to start the test, and after 1 ms, a turn-off signal was sent out.

As can be seen in Fig. 14, the inner and outer windings voltages are almost identical before the SSCB prototype is turned off. During the current interruption, the rate of decrease of the outer winding voltage is greater than that of the inner winding voltage. This means that the outer winding has a better recovery performance compared to the inner winding, which is because of the larger surface contact area between the outer winding and the LN_2 [32]. The larger contact area can increase the heat conduction from the HTS tape to surrounding LN_2. The maximum reverse voltages applied to the outer and inner windings reach −12.8 V and −6.4 V, respectively, which are much lower than the results in Fig. 13. Hence, the SSCB prototype combined with the low inductance SFCL coil has a better performance during current interruption.

3.4.3. Overcurrent detection testing

Due to the high voltage induced by the high inductance SFCL coil during the current interruption tests, the SSCB prototype with the low inductance SFCL coil is selected as the protection solution. The control block was set to Mode 3, and the threshold of the detected current was set to 1000 A. Once the mean value of the current detected by the external LEM current transducer is higher than this threshold level, a turn-off signal will be sent to the SSCB prototype.

In this test, the capacitor was pre-charged to 300 V and the result is shown in Fig. 15. The fault current starts to rise when the circuit is triggered at 0 ms. The prospective fault current is 3089 A without the SFCL, this fault current level exceeds the interruption capability of the SSCB. The SFCL coil limits the maximum fault current to 1208A, which is higher than the fault detection current level. When the current reaches 1000 A, the solid-state circuit breaker clears the fault current. The fault current is reduced from 1000 A to zero in 50 μs. After the interruption, the voltage across the SSCB prototype is equal to the capacitor voltage. The protection solution with the automatic overcurrent detection function can reduce the fault current significantly and then interrupt the fault current in a timely manner. In this section, current amplitude is used to determine the fault. In practical applicaion, the rate of rise of fault current and SFCL coil voltage can also be used for automatic fault interruption.

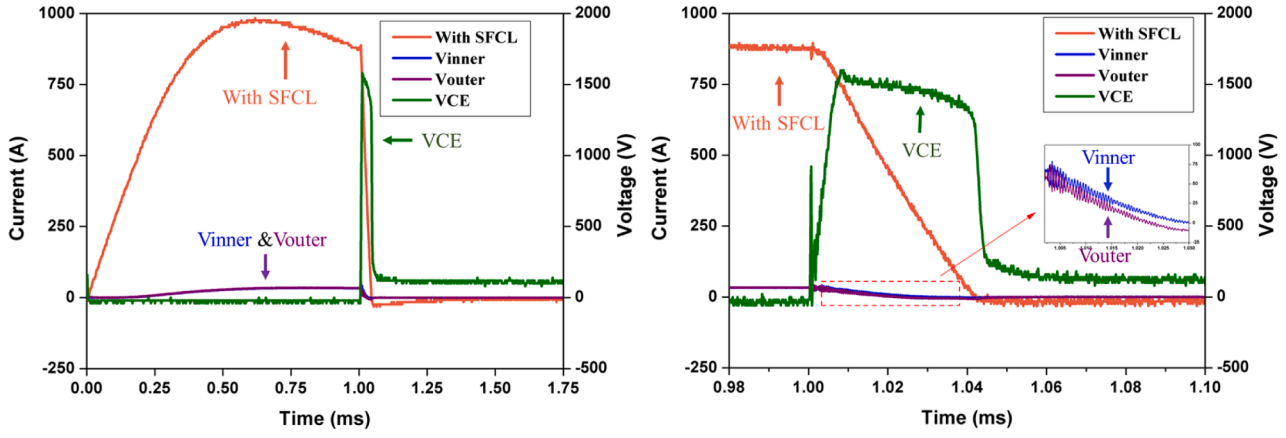

(a) Whole period (b) Zoom in during interruption

Fig. 14. Current interruption performance of the SSCB prototype with the low inductance SFCL coil at 872 A (pre-charged capacitor voltage is 200 V and the SSCB prototype is turned off at 1 ms).

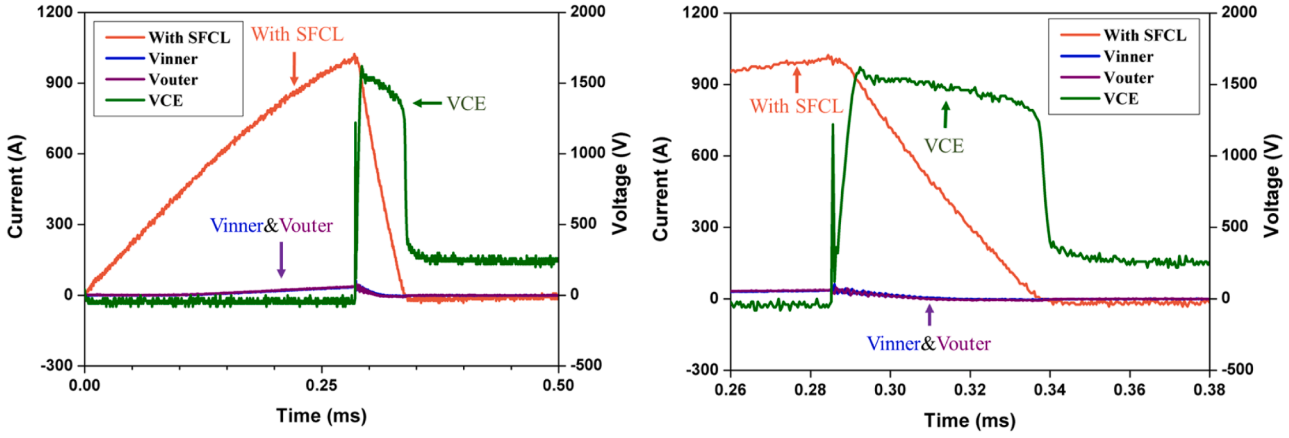

(a) Whole period (b) Zoom in during interruption

Fig. 15. Current interruption performance of the SSCB prototype with the low inductance SFCL coil using LEM current detection (pre-charged capacitor voltage is 300 V).

4. Conclusions

A DC protection solution for electric aircraft using an SFCL integrated with a DC SSCB is proposed and experimentally tested. An SFCL prototype is designed and manufactured using AMSC type 8602 HTS tape after careful selection. The responses of the SFCL coil with low and high inductance connections under different fault current levels without current interruption are investigated. Both connections can effectively limit a fault current from over 2000 A to below 1000 A. The SFCL coil with a high inductance connection can perform current limiting performance at all the current levels by limiting the rate of rise of the fault current. The difference in the current limiting ratios of the high inductance and low inductance connection methods becomes smaller as the prospective fault current increases as the quench resistance dominants the current limiting performance.

The interruption performance of the SSCB using the low inductance and high inductance SFCL coils are studied. High voltages induced by the high inductance SFCL coil has to be carefully considered during the current interruption, in particular for high voltage application. The SSCB prototype with a low inductance SFCL coil is a preferable solution to limit and interrupt fault current in DC networks, as the induced voltages across the low inductance coil windings are much lower when the current is interrupted. With overcurrent protection solution, the fault current is limited to a lower level by the low inductance SFCL prototype and then the SSCB prototype successfully detected and performed the interruption at 1000 A within 50 μs, while without the SFCL coil, the prospective fault current could reach 3089 A. With the effetive current limitation of SFCL, the current interruption rating of the SSCB can be significantly reduced and has great potnetial to achive higher power desnsity DC network protection.

CRediT authorship contribution statement

Jiawen Xi: Conceptualization, Validation, Data curation, Investigation, Writing – original draft. **Xiaoze Pei:** Conceptualization, Methodology, Validation, Supervision, Writing – review & editing. **Wenjuan Song:** Methodology. **Liyong Niu:** Methodology. **Yuhan Liu:** Writing – review & editing. **Xianwu Zeng:** Conceptualization, Methodology, Investigation.

Declaration of Competing Interest

This work is funded as part of the UK EPSRC: Developing superconducting fault current limiters (SFCLs) for distributed electric propulsion aircraft: EP/S000720/1, and the UK Royal Society International Exchanges 2018 Cost Share (China): Advanced DC fault protection by integration of superconducting fault current limiter (SFCL) with DC circuit breaker: IEC\NSFC\181111.

References

[1] MJ, Armstrong, M, Blackwelder, A, Bollman, C, Ross, A, Campbell, C, Jones, et al. Architecture, voltage, and components for a turboelectric distributed propulsion electric grid. 2015.
[2] Jones CE, Norman PJ, Galloway SJ, Armstrong MJ, Bollman AM. Comparison of candidate architectures for future distributed propulsion aircraft. IEEE Trans Appl Supercond 2016;26:1–9.
[3] Wheeler P, Bozhko S. The more electric aircraft: technology and challenges. IEEE Electrif Mag 2014;2:6–12.
[4] Schefer H, Fauth L, Kopp TH, Mallwitz R, Friebe J, Kurrat M. Discussion on electric power supply systems for all electric aircraft. IEEE Access 2020;8:84188–216.
[5] Barzkar A, Ghassemi M. Electric power systems in more and all electric aircraft: a review. IEEE Access 2020;8:169314–32.
[6] Fletcher S, Norman P, Galloway S, Burt G. Determination of protection system requirements for DC unmanned aerial vehicle electrical power networks for enhanced capability and survivability. IET Electr Syst Transp 2011;1:137–47.
[7] Barnes M, Vilchis-Rodriguez DS, Pei X, Shuttleworth R, Cwikowski O, Smith AC. HVDC circuit breakers–a review. IEEE Access 2020;8:211829–48.
[8] Pei X, Cwikowski O, Vilchis-Rodriguez D, Barnes M, Smith A, Shuttleworth R. A review of technologies for MVDC circuit breakers. In: Industrial Electronics Society, IECON 2016–42nd Annual Conference of the IEEE: IEEE; 2016. p. 3799–805.
[9] Cwikowski O. Synthetic testing of high voltage direct current circuit breakers. University of Manchester; 2016. PhD Thesis.
[10] Franck CM. HVDC circuit breakers: a review identifying future research needs. IEEE Trans Power Delivery 2011;26:998–1007.
[11] Xi J, Pei X, Zeng X, Niu L. Design, modelling, and test of a solid-state main breaker for hybrid DC circuit breaker. In: 2020 22nd European Conference on Power Electronics and Applications (EPE'20 ECCE Europe): IEEE; 2020. p. 1–10.
[12] Yazdani-Asrami M, Staines M, Sidorov G, Davies M, Bailey J, Allpress N, et al. Fault current limiting HTS transformer with extended fault withstand time. Supercond Sci Technol 2019;32:035006.
[13] Li B, He J. Studies on the application of R-SFCL in the VSC-Based DC distribution system. IEEE Trans Appl Supercond 2016;26:1–5.
[14] Pei X, Smith AC, Barnes M. Superconducting fault current limiters for HVDC systems. Energy Procedia 2015;80:47–55.
[15] Zhou G, Han M, Filizadeh S, Cao X, Huang W. Studies on the combination of RSFCLs and DCCBs in MMC-MTDC system protection. Int J Electr Power Energy Syst 2021;125:106532.
[16] Xi J, Pei X, Song W, Xiang B, Liu Z, Zeng X. Experimental tests of DC SFCL under low impedance and high impedance fault conditions. IEEE Trans Appl Supercond 2021;31:1–5.
[17] Sun J, Du J, Li Y, Mo S, Cai Y, Yuan W, et al. Design and performance test of a 20-kV DC superconducting fault current limiter. IEEE Trans Appl Supercond 2020;30:1–5.
[18] Qiu Q, Xiao L, Zhang J, Zhang Z, Song N, Jing L, et al. Design and test of 40-kV/2-kA DC superconducting fault current limiter. IEEE Trans Appl Supercond 2020;30:1–5.

[19] Song M, Dai S, Sheng C, Zhong L, Duan X, Yan G, et al. Design and tests of a 160-kV/1-kA DC superconducting fault current limiter. IEEE Trans Appl Supercond 2021;31:1–7.
[20] Song M, Sheng C, Ma T, Huang Y, Yang C, Xin Y, et al. Current limiting tests of a prototype 160 kV/1 kA resistive DC superconducting fault current limiter. Supercond Sci Technol 2020;34:014002.
[21] Xiang B, Gao L, Luo J, Wang C, Nan Z, Liu Z, et al. A CO2/O2 mixed gas DC circuit breaker with superconducting fault current-limiting technology. IEEE Trans Power Delivery 2020;35:1960–7.
[22] Xiang B, Liu Z, Wang C, Nan Z, Geng Y, Wang J, et al. DC interrupting with self-excited oscillation based on the superconducting current-limiting technology. IEEE Trans Power Delivery 2017;33:529–36.
[23] Xiang B, Gao L, Liu Z, Geng Y, Wang J. Short-circuit fault current-limiting characteristics of a resistive-type superconducting fault current limiter in DC grids. Supercond Sci Technol 2020;33:024005.
[24] Pei X, Cwikowski O, Smith AC, Barnes M. Design and experimental tests of a superconducting hybrid DC circuit breaker. IEEE Trans Appl Supercond 2018;28.
[25] Song W, Pei X, Xi J, Zeng X. A novel helical superconducting fault current limiter for electric propulsion aircraft. IEEE Trans Transp Electrif 2020;7:276–86.
[26] Song W, Pei X, Alafnan H, Xi J, Zeng X, Yazdani-Asrami M, et al. Experimental and simulation study of resistive helical HTS fault current limiters: quench and recovery characteristics. IEEE Trans Appl Supercond 2021;31:1–6.
[27] Noe M, Hobl A, Tixador P, Martini L, Dutoit B. Conceptual design of a 24 kV, 1 kA resistive superconducting fault current limiter. IEEE Trans Appl Supercond 2011; 22:5600304.
[28] Hobl A, Goldacker W, Dutoit B, Martini L, Petermann A, Tixador P. Design and production of the ECCOFLOW resistive fault current limiter. IEEE Trans Appl Supercond 2013;23:5601804.
[29] Zhang Z, Yang J, Qiu Q, Zhang G, Lin L. Research on resistance characteristics of YBCO tape under short-time DC large current impact. Cryogenics 2017;84:53–9.
[30] J, Janesch, Two-wire vs. four-wire resistance measurements: Which configuration makes sense for your application. 2013. p. 2-4.
[31] Xi J, Pei X, Niu L, Feehally T, Wilson P, Gu C, et al. A solid-state circuit breaker for DC system using series and parallel connected IGBTs. Int J Electr Power Energy Syst 2022;139:107996.
[32] Yazdani-Asrami M, Staines M, Sidorov G, Eicher A. Heat transfer and recovery performance enhancement of metal and superconducting tapes under high current pulses for improving fault current-limiting behavior of HTS transformers. Supercond Sci Technol 2020;33:095014.